# A new standard for line-scale calibrations in the Netherlands

***Extremely accurate calibration of (line) scales requires dedicated equipment and measurement conditions that are usually only implemented at the national metrology institutes. The Dutch metrology institute VSL has several facilities to calibrate scales from small micrometer scales up to leveling rods and tape measures with lengths over tens of meters to high accuracy. In order to ensure that VSL can continue to provide services for the ever increasing demand for higher accuracies, these facilities are continuously improved. This paper describes the efforts that have been undertaken recently to improve VSL's capabilities for the calibration of high-precision line scales as well as the motivation for the choices that have been made during this process.***

• *Richard Koops, Ancuta Mares and Jan Nieuwenkamp* •

Line scales are important physical standards of length, used for accurate positioning or measurement in one, two or three dimensions. Depending on the application, line scales can have dimensions from fractions of a millimeter to several tens of meters. For example, small scales are used to calibrate the field of view of optical microscopes. Scales with dimensions in the meter range are used to read out the position of machine tools and measuring machines, while leveling rods find their use in geodetic surveying.

## Calibration of high-precision line scales

Until recently, precision lines scales were calibrated manually at VSL using a 400 mm SIP measuring machine,

**Authors' note**

Richard Koops and Ancuta Mares work in the Research and Development department of VSL, formerly NMi Van Swinden Laboratorium, in Delft, the Netherlands. Jan Nieuwenkamp works in the Calibration and Reference Materials department of VSL. The authors acknowledge the financial support of the Dutch Ministry of Economic Affairs.
More information:
mvveghel@vsl.nl (Marijn van Veghel)
www.vsl.nl

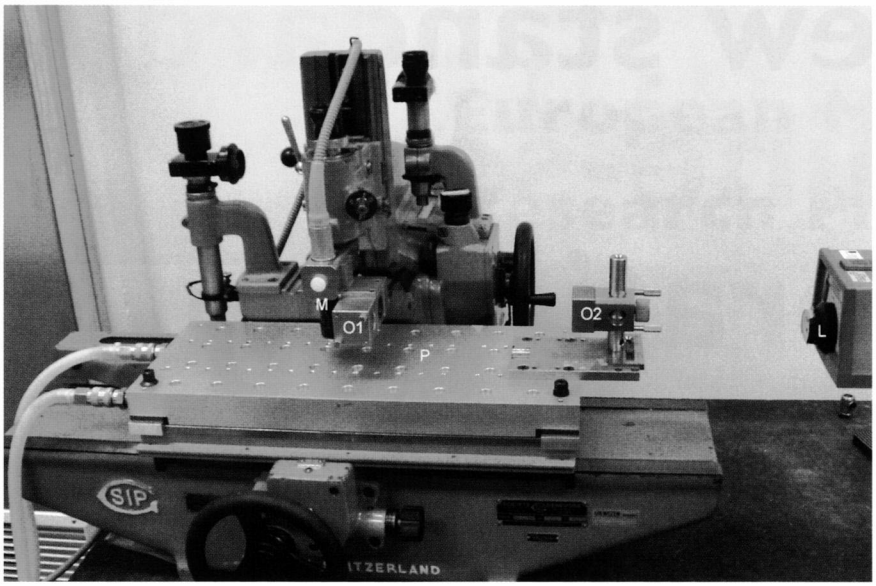


Figure 1. Previous facility at VSL to manually calibrate line scales up to 400 mm. The position of the platform P with the scale (not shown) is manually translated with respect to a video microscope M and measured by a laser interferometer consisting of laser L and optical components O1 and O2. For improved temperature stability the temperature of the platform can be controlled separately.

see Figure 1. Although this machine has three axes, only one of them is used during the calibration process. The measuring machine is equipped with a camera system to visualize the scale markers and a laser interferometer system to measure the position of the camera relative to the scale.
During the calibration procedure the image from the camera is converted to a single curve that represents the intensity of the image features – manual alignment of the scale marker to the exact centre of the image is performed by adjusting this curve to its mirror image. After each alignment step the position of the camera with respect to the scale is stored manually.
The uncertainty that has been realized by this facility and that is registered as part of VSL's calibration and measurement capabilities in the CMC database at BIPM [1] is 100 nm + $10^{-6}L$ where $L$ is the length of the scale.

During the past decade this facility has been upgraded, but due to mechanical, optical, thermal and electronic limitations further improvements are not feasible without major modifications. Additionally, this facility has the drawback that it requires realignment of the entire optics for the laser interferometer for each scale. Finally, given the fact that a large part of the calibration procedure is performed manually, the amount of scale markers that can be calibrated is limited due to time constraints.

## New calibration set-up

In order to improve the quality for precision line-scale calibrations, it was therefore decided to design and build a new facility. This facility should enable lowering the measurement uncertainty to 30 nm + $5{\cdot}10^{-7}L$ for an increased measurement range of 1,000 mm. To minimize the manual labour during the calibration process, the measurement sequence should be fully automated, allowing calibration of every marker on the line scale. The basic design concept chosen for the new line-scale set-up is similar to that realized at the Finnish metrology institute MIKES [2].

A schematic overview of the new set-up is shown in Figure 2. The system can be divided into four main parts: a granite guide, an actuation mechanism, a movable vision system and a laser interferometer. The vision system captures images of the scale markers on the fly while moving over the line scale on an air-bearing platform that is translated by the actuation mechanism. Along with the image acquisition of the line-scale markers the position of the vision system is captured synchronously by a laser interferometer. In the following sections the individual components will be described in more detail.

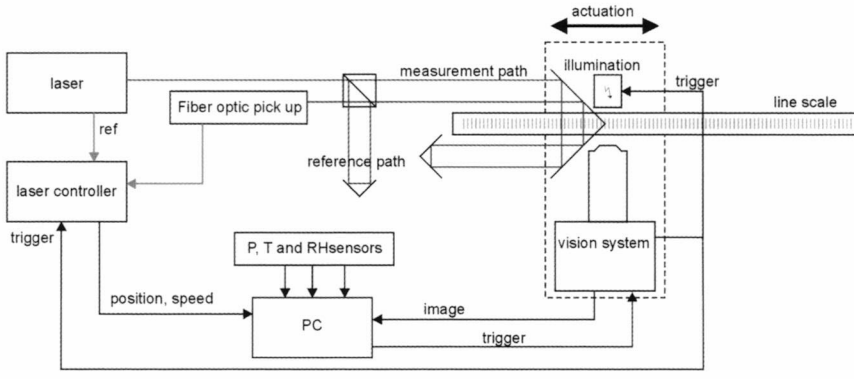


Figure 2. Schematic view of the new set-up. The vision system is mounted on an air-bearing platform that is connected to a motor by a wire. The position of the platform with respect to the stationary line scale is measured by a laser interferometer.

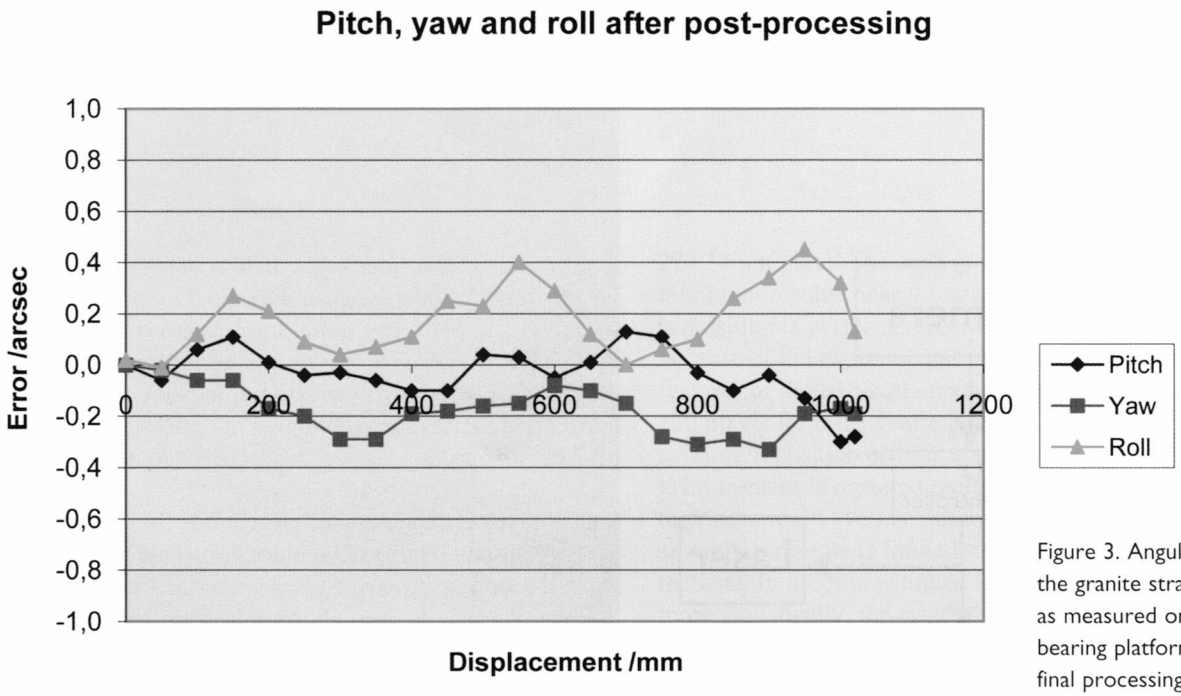


Figure 3. Angular errors of the granite straight guide as measured on the air-bearing platform after the final processing step.

## Granite straight guide

The straight guide is part of a granite stone measuring 2,000 x 1,000 x 400 mm$^3$. The straight guide defines the movement of the air-bearing platform that holds the vision system. Shape deviations in the guide result in pitch, yaw and roll motion of the air-bearing platform and therefore result in changes in the directions of view of the vision system. Especially pitch rotates the view in the direction of measurement resulting in a measurement error. Given the total measurement uncertainty for the complete set-up, VSL's requirement for the maximum angular errors (pitch, yaw and roll) is 0.4 arcsec (approximately 2 µrad), which was met after the granite guide was post-processed by the supplier [3] in the VSL laboratory; see Figure 3.

The thickness of the granite was determined by the boundary condition for the stability of the entire set-up. When the granite deforms due to the moving platform, the supporting points of the scale will pivot and translate the scale during the calibration. A constraint of 2 nm for the maximum displacement of the scale restricts the bending of the granite to 30 nm, resulting in a thickness of the granite block of 400 mm.

During calibration the line scale is supported at the Bessel points, ensuring minimal change in the length of the scale. Since the remaining bending of the granite will result in opposite pivoting of the supports, the scale might slip on the contact points and change the position of the scale with respect to the measurement system in a non-reversible way. To avoid this, materials with different friction coefficients for the two supporting points were selected.

The stability of granite reference flats is largely determined by the stability of the vertical temperature gradient along the thickness of the granite [4]. A vertical temperature gradient of 0.1°C will result in a flatness error of about 1 µm that produces 1 µrad angular error over 1,000 mm. Therefore, besides conditioning the laboratory, the power dissipation in and around the set-up should be kept to a minimum. This was achieved by using low-power components (high-efficiency LED [5, 6] in pulsed mode, low-power dc motors [7]) and placing the dissipating equipment outside the measurement area.

## Actuation

The air-bearing platform is translated over the full range of 1,000 mm using a kevlar wire that is connected to a low-power dc motor [7]. The air supply is connected to the platform by relatively stiff plastic tubing. During the travel over 1,000 mm these tubes change shape and therefore exert changing forces on the platform that could distort the linear translation. In order to avoid this, a second, smaller platform on a conventional ball-bearing guide was realized that moves synchronously to the main platform to stabilize the shape of the tubing and ensure that the movement of the main platform is not distorted.

## The measurement system

During the calibration sequence, the measurement platform with the vision system is moving continuously. The position of the scale markers is calculated from both the image information and the position information, so it is very important that these two are acquired synchronously. The data-acquisition timing scheme is shown in Figure 4.

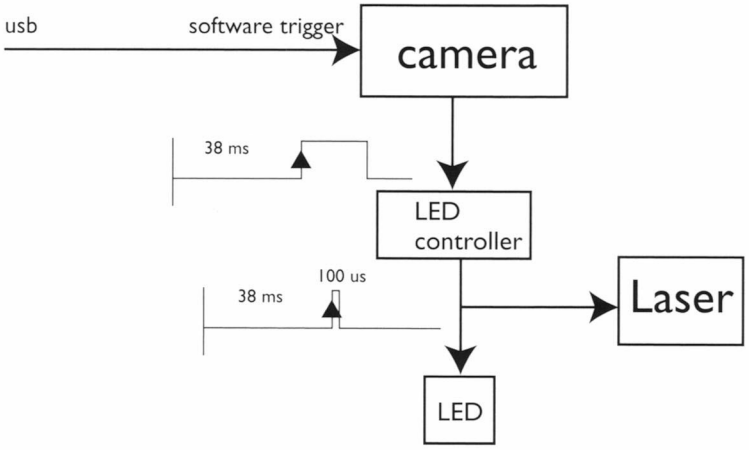


Figure 4. The synchronization of the data acquisition is critical and is initiated by a software trigger of the camera of the vision system. The camera has to prepare for acquisition and after 38 ms releases a trigger that starts the LED flash illumination and latches the momentary position information of the laser interferometer. The trade-off between acceptable image blurring and sufficient exposure of the frame has finally resulted in an optimized flash duration of 100 µs.

The vision system consists of a microscope with zooming capability [8] and a camera [9] with a resolution of 1,280 pixels x 1,024 pixels. The microscope is equipped with a quarter-wave plate to maximize the contrast of the relevant features on the line scales. The field of view at the highest magnification setting is about 0.28 x 0.35 mm$^2$, yielding about 270 nm per pixel. Initial image analysis is performed using a basic algorithm on-line during the measurement, in order to detect errors of the calibration process itself. A more detailed analysis with higher accuracy is performed off-line, because this is computationally too intensive.

Since the measurement takes place while the vision system is moving, the image will be blurred to some extent. Only when the camera has a very fast shutter or when the illumination time is short enough, the blurring will become acceptable. It was decided to use pulsed illumination – for an acceptable image contrast it was observed that a pulse duration of at least 100 µs is necessary. For the measurement speed of 0.2 mm/s the blurring therefore becomes 20 nm. Since the blurring should be equal for every scale marker it does not contribute directly to the measurement uncertainty. It is the fluctuations in the actual measurement speed, determined to be about 10% of the speed, which will cause different blurring for different markers. The final contribution due to image blurring to the measurement uncertainty is therefore 2 nm.

The image acquisition during the calibration process is adjusted such that the relevant information of the scale marker is close to the centre of the image, in order to minimize the influence of measurement errors due to the

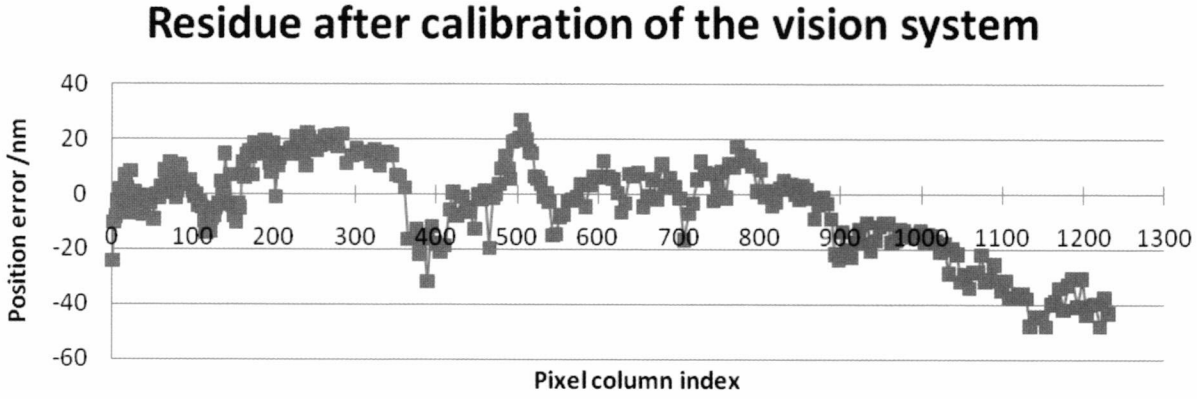


Figure 5. The residual errors of the vision system after calibration with the laser interferometer along all pixel columns. The graph shows slightly less columns than the actual 1,280 because for the first and last few columns the line-scale marker is not completely imaged. The calibration has been optimized for the central region of the vision system between pixel columns 540 and 740.

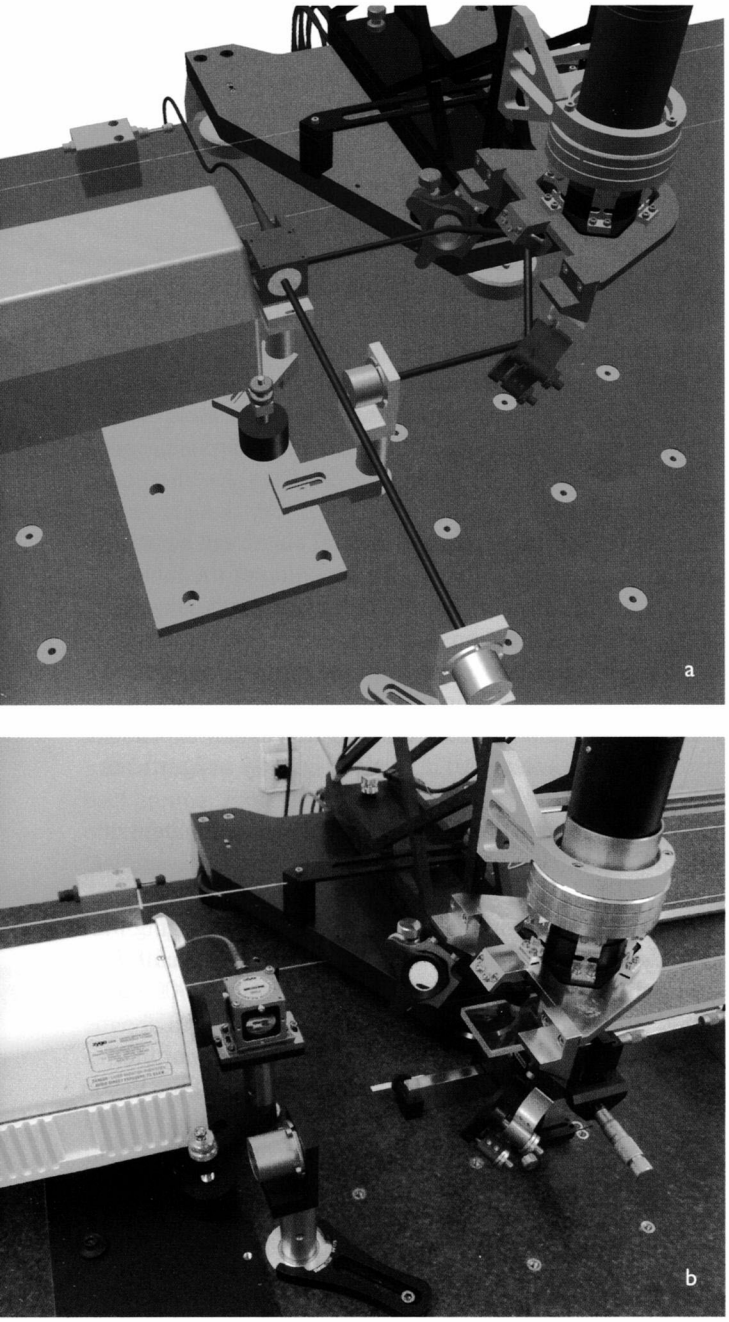


Figure 6. Design (a) and realization (b) of the measurement system. The laser beams along the measurement and reference path have been indicated in the design drawing. The effective measurement position of the laser interferometer is aligned to the field of view of the vision system in order to minimize the Abbe error.

inhomogeneous illumination and aberrations of the imaging system. In order to convert the image information, stated in pixels, to a position in meters, the vision system was calibrated by translating a marker line across the entire field of view. Figure 5 shows the residue of the position for every pixel column of the vision system that was obtained after subtracting the linear response for a scaling factor of 277.34 nm/pixel. The scaling factor was calculated for a minimum residue near the center of the image. The image acquisition is performed between the columns 540 and 740, because of the experimental observation that the relevant features of the line-scale markers are always imaged within 100 pixels from the centre position at column 640. Here the maximum position error is about 15 nm. If the measurement is repeated multiple times the contribution to the error would average out to less than 1 nm. Since the amount of repeats is limited, the fully averaged value is not realistic. In order to estimate the uncertainty contribution more realistically, the standard deviation of the errors in the centre region is taken. This value is 7 nm.

The position of the air-bearing platform with the vision system is measured with a double-pass laser interferometer [10], shown in Figure 6, for which most components are commercially available. For the speed that is used only one image can be taken with the scale marker close to the centre of the frame. To ensure sufficient signal quality the image processing uses averaging over all 1,024 image lines. The contribution to the measurement uncertainty due to the laser interferometer is given by its resolution of 0.6 nm.

The laser interferometer signal is optimized using high-quality mirrors and maximum mechanical and thermal stability of the optical components in the interferometer. Also the connection between the composite cube corner and the vision system has to be thermally stable. A temperature fluctuation of 0.1 K would result in an error in the scale calibration of at least 100 nm for a direct mount of the two components. In order to reduce this error, a symmetric invar mount was constructed with its thermal centre nominally on the symmetry axis of the microscope, reducing the contribution to the measurement uncertainty to 10 nm.

During a line-scale calibration the starting position is such that the vision system is closest to the laser interferometer optics, minimizing the amount of air in the measurement path and therefore maximizing the stability of the zero-position measurement. Additionally, the interferometer was designed to have equal lengths of the measurement path and the reference path at the starting position of the calibration (see Figure 6), such that most local fluctuations will cancel out.

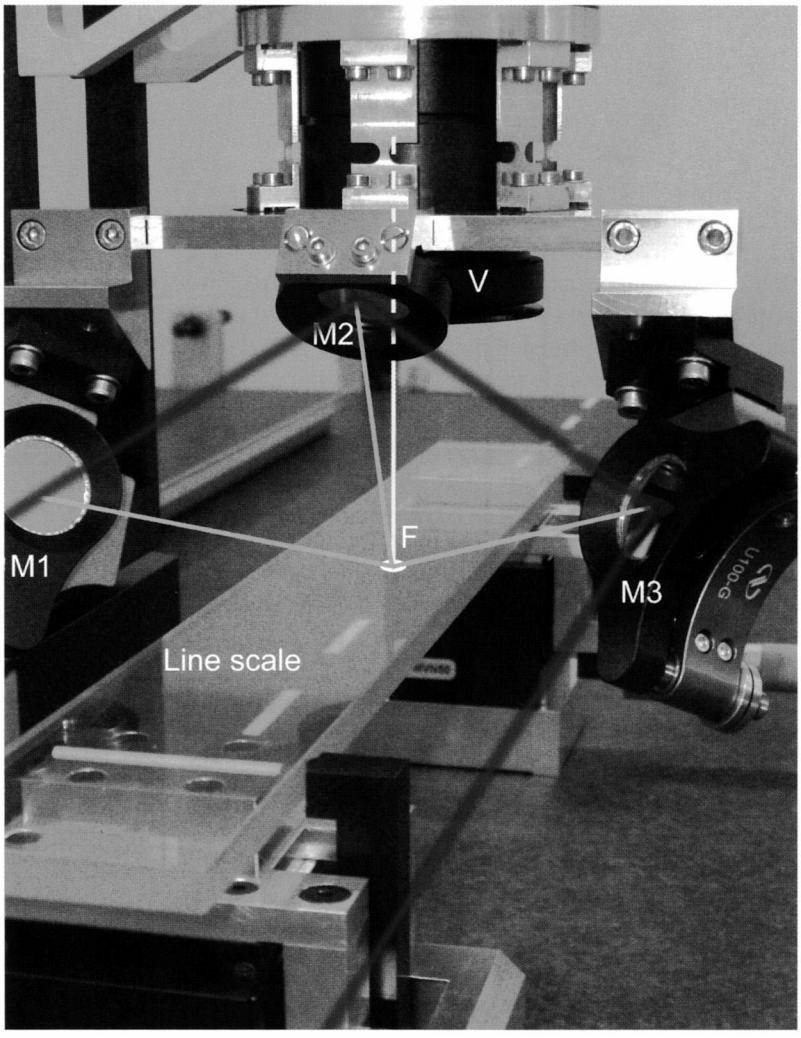


Figure 7. The composite cube corner retroreflector consisting of mirrors M1, M2 and M3 has its virtual apex aligned at the centre of the focal plane F of the vision system V. Rotational errors of the vision system during the translation result in a tilt of the field of view. The resulting errors as measured by the vision system are, however, compensated because the cube corner apex is translated over the same distance.

## Abbe errors

Since the accuracy of the straight guide is limited by the residual imperfections that remain after post-processing the granite, the translation of the platform is not perfectly straight. The Abbe error that is introduced in this way is proportional to the tilt of the vision system and the distance between the vision system and the line scale. An Abbe error compensation was implemented as shown in Figure 7. The optical system is implemented as a composite cube corner retroreflector that has the apex at the effective point of measurement. In this way any common movement of this point and the cube corner can be recorded accurately, irrespective of residual rotations during the movements. The cube corner was implemented containing three separate mirrors that are mutually perpendicular and define an apex where their planes intersect. This apex is positioned at the centre of the focal plane of the vision system. In practice the positioning can be done with finite accuracy, typically 1 mm, yielding an Abbe residue of 2 nm.

## Cosine errors

The line-scale facility requires several alignment steps to minimize cosine errors. First, the deviation of the three mirrors in the cube corner from mutual perpendicularity causes different directions between the exit beam and the incoming beam. The alignment of the mirrors has been optimized using VSL's angle calibration facility to less than 7 arcsec. This results ultimately in a length-dependent error of approximately $10^{-9}L$, which is nearly insignificant.

The second source of cosine errors is the misalignment of the line scale to the translation direction. The final angular accuracy of alignment is determined by the length of the scale. Given the position accuracy of 1 µm when using the vision system, the cosine error ranges from about $5{\cdot}10^{-7}L$ for small scales to less than $10^{-12}L$ for scales of 1,000 mm.

The third source of cosine errors is the alignment of the laser interferometer to the translation direction of the vision system. This alignment is inspected by tracking the position of the retroreflected laser beam with a position-sensitive detector as the platform is moving. The alignment is then optimized by changing the laser position to reduce the position shift of the returning beam to less than 50 µm, resulting in a cosine error of about $10^{-9}L$.

## Repeatability

The repeatability has been established by comparing sequential data without changing the alignment and the other measurement parameters like speed and illumination. It was studied separately how the measured positions of the scale markers depend on the amount of light and on out-of-focus conditions. This dependence was found to be not significant. This is to be expected, since the conditions are the same for every line-scale marker and only the relative positions of the scale markers with respect to the zero markers are finally calculated.

In order to minimize the influence of environmental conditions during the repeatability measurements, the zero

marker of the line scale for which the lengths of the interferometer paths are shortest was used. Also, at a single point the measurement could be repeated many times in contrast to the situation when the vision system is moving and only one data point can be taken with the marker image centered in the frame. The repeatability under these conditions was established to be 8.2 nm and is probably overestimated since it partly contains the calibration residue of the vision system.

## Data processing

The data analysis is based on combining the position information from the laser interferometer and the image information from the vision system. For a simple line-scale marker the image is a straight vertical line of a certain width, usually imaged as a bright feature on a dark background. First, all horizontal image lines are added, obtaining a curve proportional to the average intensity of the line-scale marker image. The centre position is calculated from the average of the positions of the left and right edge. These positions in turn are defined as the interpolated positions at 50% of the height of the intensity curve. The average of the positions of the left and right edge is finally converted from pixels to meters using the calibration factor of the vision system.

The second part of the position information is generated by the laser interferometer. Here also some processing is required before this becomes a traceable value. The raw position counts as generated by the laser interferometer are converted to meters based on the calibrated wavelength, the interpolation factor of the laser controller, the correction for the momentary index of refraction and the material temperature of the line scale.

Lasers used by VSL are calibrated in-house using either a iodine-stabilized standard laser or more directly against VSL's frequency comb. These calibrations result in a very accurate knowledge of the frequency of the laser light. The vacuum wavelength is calculated using the definition of the speed of light ($c$ = 299 792 458 m/s [11]). When the laser is used under ambient conditions, the wavelength is changed by the refractive index of air. Since direct measurement of the refractive index is difficult, the correction is usually done by calculating the index using the Edlén equation [12] while constantly measuring the required parameters, such as air pressure, air temperature, relative humidity and $CO_2$ content. The validity of the Edlén model to calculate the index of refraction is limited to about $1 \cdot 10^{-8}$, putting a lower limit on the accuracy. The uncertainty in the distance measurement is also determined by the uncertainty in the values of the ambient parameters, adding up to $5 \cdot 10^{-8} L$.

Besides the correction due to ambient air conditions the length of the line scale also depends on its temperature. The correction is calculated based on the coefficient of thermal expansion and the temperature deviation from 20 °C. When the thermal expansion coefficient is not explicitly calibrated, an uncertainty of $10^{-6}$ $K^{-1}$ in its value is assumed. With a temperature gradient over the scale estimated to be 0.1 K, the relative contribution to the measurement uncertainty is $10^{-7} L$.

Combining the processed laser interferometer and image information finally results in an accurate position of each line-scale marker.

## Uncertainty budget

The most significant uncertainty sources have been identified in the previous sections, resulting in the uncertainty budget as presented in Table 1.

Table 1. Uncertainty budget.

| Source | Uncertainty | Distribution | Standard uncertainty |
|---|---|---|---|
| Laser interferometer | 0.6 nm | rectangular | 0.2 nm |
| Vision system | 7 nm | normal | 7 nm |
| Data synchronisation | 2 nm | rectangular | 1.2 nm |
| Abbe error static | 2 nm | rectangular | 1.2 nm |
| Abbe error dynamic | 1 nm | rectangular | 0.6 nm |
| Laser alignment | $1.2 \cdot 10^{-9} L$ | rectangular | $7 \cdot 10^{-10} L$ |
| Scale alignment | $1.2 \cdot 10^{-9} L$ | rectangular | $7 \cdot 10^{-10} L$ |
| Edlén equation | $1 \cdot 10^{-8} L$ | normal | $1 \cdot 10^{-8} L$ |
| Refractive index | $5 \cdot 10^{-8} L$ | normal | $1 \cdot 10^{-8} L$ |
| Expansion correction | $1 \cdot 10^{-7} L$ | rectangular | $6 \cdot 10^{-8} L$ |
| Deformation granite | 2 nm | normal | 2 nm |
| Retroreflector alignment | $1 \cdot 10^{-9} L$ | normal | $1 \cdot 10^{-9} L$ |
| Retroreflector stability | 10 nm | rectangular | 5.8 nm |
| Repeatability | 8.2 nm | normal | 8.2 nm |
| Combined standard uncertainty | | | 12.5 nm + $7.9 \cdot 10^{-8} L$ |
| Expanded uncertainty (95% coverage) | | | 25 nm + $1.6 \cdot 10^{-7} L$ |

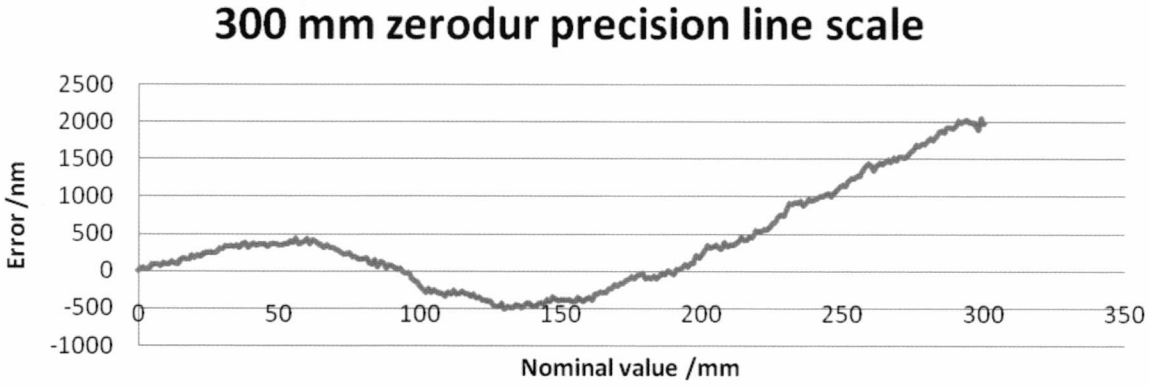


Figure 8. One of the first results obtained with the new set-up for VSL's 300 mm Zerodur precision line scale, showing the errors for every single line-scale marker along the scale. This scale has a deliberate, large deviation from nominal towards the end of the scale but was previously calibrated only at a few points.

## First results

Figure 8 shows the result of one of the first fully automated measurements on VSL's 300 mm Zerodur precision line scale. The result is an average over two measurement sequences moving the vision system in opposite directions. Although from this result it had to be concluded that the alignment of the laser to the translation direction still had to be improved, the graph shows the errors for all of the 300 individual line-scale markers for the first time and reveals a regular substructure that was previously unknown and could indicate imperfections in the equipment that was used to manufacture the scale.

The new line-scale set-up will be validated completely in the coming months by comparison to results from other metrology institutes.

## Conclusion

The new facility for line-scale calibrations at VSL has been described in detail and first results were demonstrated. This facility will provide internationally accepted calibration services at a much reduced uncertainty level, covering all individual markers for line scales up to 1,000 mm.

## References

[1] The calibration and measurement capabilities are publicly available via kcdb.bipm.org/AppendixC.

[2] A. Lassila, E. Ikonen, K. Riski, Interferometer for calibration of graduated line scales with a moving CCD camera as a line detector. *Applied Optics*, Vol. 33, 18 (1994).

[3] Q-Sys custom-made granite straight guide and air-bearing platform, www.q-sys.eu.

[4] Raad voor Accreditatie, 'RvA-I4.03: Temperatuur- en vocht-invloeden bij vlakplaatmetingen (in Dutch), www.rva.nl.

[5] CCS / HLV-24 SW NR-3W white LED.

[6] Gardasoft LED controller PP520F.

[7] Maxon S 2332.966 12V dc motor.

[8] Leica Z16 APO zoom microscope.

[9] Edmund optics EO-1312 1280x1024 pixels black and white CMOS camera.

[10] Zygo ZMI 2000 laser head and 2400 measurement board.

[11] Resolution 1 of the 17th meeting of the CGPM (1983), www.bipm.org.

[12] K.P. Birch, M.J. Downs, Correction to the Updated Edlén equation for the refractive index of air, *Metrologia*, 1994, 31, 315-316.